Coal Combustion and Gasification Products is an international, peer-reviewed on-line journal that provides free access to full-text papers, research communications and supplementary data. Submission details and contact information are available at the web site.

© 2009 The University of Kentucky Center for Applied Energy Research and the American Coal Ash Association

Web: www.coalcgp-journal.org

ISSN# 1946-0198

Volume# 1 (2009)

Editor-in-chief: Dr. Jim Hower, University of Kentucky Center for Applied Energy Research

CCGP Journal is collaboratively published by the University of Kentucky Center for Applied Energy Research (UK CAER) and the American Coal Ash Association (ACAA). All rights reserved.

The electronic PDF version of this paper is the official archival record for the CCGP journal.

The PDF version of the paper may be printed, photocopied, and/or archived for educational, personal, and/or non-commercial use. Any attempt to circumvent the PDF security is prohibited. Written prior consent must be obtained to use any portion of the paper's content in other publications, databases, websites, online archives, or similar uses.

Suggested Citation format for this article:

Valentim, B., Guedes, A., Flores, D., Ward, C.R., Hower, J.C., 2009, Variations in fly ash composition with sampling location: Case study from a Portuguese power plant. *Coal Combustion and Gasification Products* 1, 14-24, doi: 10.4177/CCGP-D-09-00017.1

CCGP Coal Combustion and Gasification Products

ISSN 1946-0198

journal homepage: www.coalcgp-journal.org

Variations in fly ash composition with sampling location: Case study from a Portuguese power plant

B. Valentim[1,*], A. Guedes[1], D. Flores[1], C.R. Ward[2], J.C. Hower[3]

[1] Centro e Departamento de Geologia Faculdade de Ciências da Universidade do Porto, Rua do Campo Alegre 687, 4169-007, Porto, Portugal. bvvalent@fc.up.pt
[2] School of Biological, Earth and Environmental Sciences, University of New South Wales, Australia
[3] University of Kentucky Center for Applied Energy Research, Lexington, Kentucky

A B S T R A C T

Fly ash (FA) is a heterogeneous and complex material resulting from coal combustion in thermoelectric power plants (TPP). Therefore, different types of coals, worldwide, produce FAs with different compositions. However, the location of the FA sampling system, inside the TPP, is also important to the composition of the FA produced at each location. A case study of FA from a Portuguese TPP, using several coal and FA characterization techniques (particle size analysis, proximate and ultimate analyses, XRF, SEM/ESEM/EDS, Optical microscopy, XRD, inferred chemistry, and AAS), has shown that FA chemical classification, mineralogy and phase-mineral classification, and trace elements (Cr, Cu, Mn, Ni, Pb, and Zn) vary due to sampling location. This has implications for improved understanding of the combustion system, as well as in collecting ash products from TPPs for particular market applications.

© 2009 The University of Kentucky Center for Applied Energy Research and the American Coal Ash Association
All rights reserved.

A R T I C L E I N F O

Article history: Received 28 October 2009; Received in revised form 4 December 2009; Accepted 9 December 2009

Keywords: fly ash; chemical classification; phase-mineral classification; trace elements

1. Introduction

Many studies refer to coal-fired-unit fly ash *sensu latu*, i.e., including all the fly ash (FA) produced during the burning of the coal, the fly ash collected by the electrostatic precipitators or the baghouses, the fly ashes sold for cement production, etc., without mentioning where the fly ashes were captured inside the thermoelectric power plant (TPP). However, the composition of fly ashes is dependent on the coal types and technological processes used in TPPs. For example, major and minor element distribution variations in fly ash in a TPP have been described (Clarke, 1993; Goodarzi, 2006; Hower et al., 2006; Huang et al., 2004; Kaakinen et al., 1975; Klein et al., 1975; Mastalerz et al., 2004; Meij, 1994).

Since fly ash is a heterogeneous and complex anthropogenic material, and, like coal, includes organic and crystalline and amorphous inorganic phases, a large number of techniques may be applied in fly ash characterization (French et al., 2007; Vassilev & Vassileva, 2005), to study FA mineralogy (Raask, 1982; Vassilev & Vassileva, 1996a; Ward & French, 2006), morphotypes (Anshits et al., 1998; Bailey et al., 1990; Fomenko et al., 1998a,b; Hower & Mastalerz, 2001; Hower et al., 2005; Sokol et al., 2002; Suarez-Ruiz & Valentim, 2007; Vassilev & Vassileva, 2007), Hg capture by carbon (Hower et al., 2000; Senior & Johnson, 2005), magnetic properties (Anshits et al., 2000; Hansen et al., 1981), the environmental and technological behavior of trace elements, the mechanisms for concentration enhancement, the relation between trace elements and fly ashes (Block & Dams, 1979; Clark, 1993; Conzemius et al., 1984; Danihelka et al., 2003; Donahoe et al., 2007; Finkelman et al., 1990; Haynes et al., 1982; Meij, 1994; Meij & Winkel, 2009; Swaine, 1990, 2000; Valkovic, 1983; Yan et al.,

* Corresponding author. *Tel.*: +351 220402474. *E-mail*: bvvalent@fc.up.pt

doi: 10.4177/CCGP-D-09-00017.1
© 2009 The University of Kentucky Center for Applied Energy Research and the American Coal Ash Association. All rights reserved.

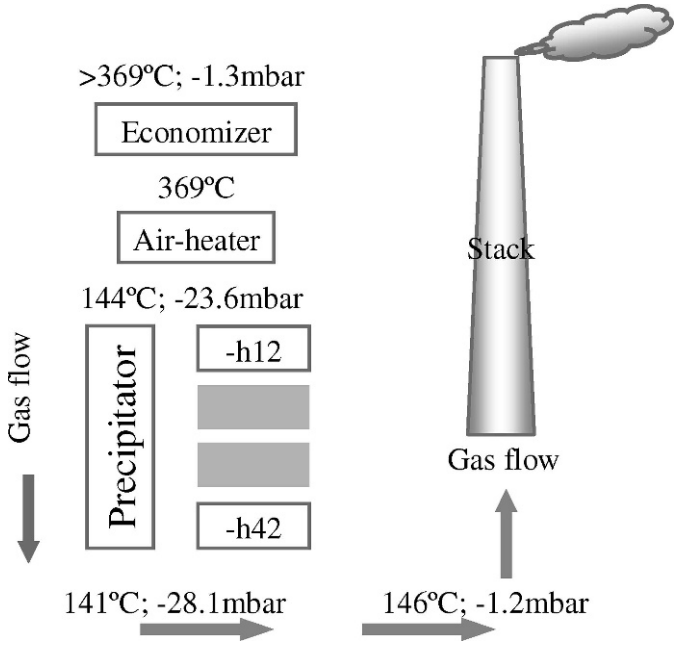

Fig. 1. Layout of sampling locations (Economizer, Air-heater, ESP-h12, and ESP-h42), flue gas temperature and pressure.

2001), and chemical classification of fly ashes (Roy & Griffin, 1982; Vassilev & Vassileva, 2007), among others. Therefore, a case study of FA from a TPP was conducted using several characterization techniques in order to see if FA variations inside a TPP are exclusive of some properties or if they cover a wide range of situations: granulometry, carbon content, major oxides and chemical classification, mineralogy and phase-mineral classification, and trace elements (Cr, Cu, Mn, Ni, Pb, and Zn).

2. Materials and methods

A Portuguese 630-MW TPP burning pulverized coal and equipped with low-NO_x burners was selected for this study. Samples of two different coals, blended at a 50:50 ratio to provide the plant feed, were collected before blending and pulverization, together with the fly ash from the Economizer, Air-heater, and the electrostatic precipitators (ESP: first line - hopper 12 - and final line - hopper 42; named ESP-h12 and ESP-h42, respectively). The sampling process was conducted for three days and, in the end, each sampling point was considered an individual sample by combining all the subsamples of that location. During this period, fly ashes were also sampled from the stack using an Andersen "Universal Stack Sampler", placed at 87.20 meters and operating isokinetically for two hours (Figure 1).

Particle size analysis for determination of the cumulative distribution at 25 μm, 45 μm, 75 μm, and 150 μm was conducted by laser granulometric methods using a Coulter LS130 Laser Granulometer apparatus. To compare the granulometric results with average Portuguese and International values, the fly ash characterization also included the fineness test of retention on a 45-μm sieve, carried out according to NP EN 451-2 1995 (ISO 565).

Proximate and ultimate analyses were conducted on the coals and fly ashes following the appropriate ASTM procedures: for coal, the ASTM D3172 proximate analysis standard was followed; ultimate analysis (C, H, and N) was carried out in a LECO CHN 2000 with total sulfur determined on a LECO-SC-144DR.

Coal petrography was evaluated using a Leitz Wetzlar incident-polarized-light microscope equipped with a 50× oil-immersion objective, wavelength (λ) retardation plate, and coupled to a Swift Model F point counter. Coal standard petrographic methods were followed (ISO 7404-3 for maceral composition, and ISO 7404-5 for vitrinite reflectance).

Total carbon and total sulfur (Leco methods), carbon species, and the Loss-on-ignition (LOI at 1000°C) of the fly ashes were determined at ACME Analytical Laboratories, Ltd.

Major oxide determinations for the fly ashes were carried out by the University of New South Wales Analytical Centre. A representative sample of each fly ash was calcined at 1050 °C and the loss on ignition determined. Each calcined ash was then fused with lithium metaborate and cast into discs (after method of Norrish and Hutton, 1969), and each disc was analyzed by X-ray fluorescence (XRF) spectrometry using a Philips PW 2400 spectrometer and SuperQ software. The results were expressed as percentages of the major element oxides in the original ash sample.

A representative portion of each coal sample was ashed at 815 °C, and the resultant ash analyzed by the same method as described above.

Trace elements (Cr, Cu, Mn, Ni, Pb, Zn) in the coal high temperature ashes (HTA at 815°C) and in the fly ashes were determined by atomic absorption spectrometry (AAS). The AAS analyses were carried out in a GBC902 instrument, using sample preparation techniques described in ASTM D3682.

Scanning Electron Microscopy (SEM) was carried out to assess to the fly ash morphotypes in detail, using a JEOL JSM-35C microscope equipped with an energy-dispersive X-ray (EDS) spectrometer analyzer (EDS NORAN-VOYAGER). Photomicrographs were obtained of the fly ash particles and semi-quantitative analysis of the elements carried out for key points within the ash particles.

The mineralogy of the coal samples was determined on low-temperature coal ashes (LTA) obtained after oxidation at 200°C in oxygen–plasma using a EMITE CHK 1050× asher. The crystalline phases in the LTA residues were identified by X-ray diffraction using a Philips PW 1830 diffractometer equipped with graphite-diffracted-beam monochromator, using CuKα radiation, 40 kV and 20 mA, and goniometer speed of 1° 2θ per minute. The proportions of the different phases in each LTA were determined from the X-ray diffractograms using the Siroquant data processing system (Taylor, 1991), based on the principles developed by Rietveld (1969).

Representative portions of four fly ash samples were finely powdered, and the mineralogy of each powdered sample was analyzed by X-ray powder diffraction in a similar way. Special techniques, based on the addition of a weighed-in proportion of a ZnO spike to each ash sample, were used as part of the Siroquant analysis procedure (Ward & French, 2006) to estimate the percentage of non-crystalline material (amorphous glass) present.

An inferred chemistry of the amorphous fraction in the fly ashes was calculated by taking away the chemistry of the crystalline phases in the ashes from the total ash chemistry, as described by Ward and French (2006).

3. Results and discussion

3.1. Feed coals

South African Kangra coal and Colombian El Cerrejon coal were the blend components for the feed coal. The properties of the two coals are summarized in Table 1.

Table 1
Coal characterization

Coal	Moisture (a.r., wt%)	Ash (d.b., wt%)	VM (d.b., wt%)	Elemental analysis (d.b., wt%)					(MJ/kg)	
				C	H	N	S			
Kangra	8.5	13.8	25.0	72.4	4.1	2.0	0.9		28.55	
El Cerrejon	5.4	12	26.6	70.1	5.5	4.3	0.9		29.01	
			Petrography							
		R_r	σ	V	L	I	MM			
Kangra		0.7	0.06	24	6	64	7			
El Cerrejon		0.6	0.06	74	3	15	8			
		High temperature (850°C) coal ash major oxides (wt%, dry basis; values normalized to 100%)								
	SiO_2	Al_2O_3	K_2O	Ti_2O	P_2O_5	CaO	MgO	Na_2O	MnO	Fe_2O_3	SO_3
Kangra	42.87	23.72	0.53	1.21	0.64	9.45	2.15	0.19	0.06	9.40	9.77
El Cerrejon	61.08	20.62	1.96	0.89	0.18	2.21	1.78	0.67	0.06	7.31	3.26
Clarke[1]	54.65	23.54	1.51	1.14	0.26	6.26	1.68	0.81	0.06	6.63	3.49
		Coal ash chemical classification (Vassilev and Vassileva, 2007)									
		SiO_2+Al_2O_3+K_2O +TiO_2 + P_2O_5		CaO+MgO+SO_3 +Na_2O + MnO		Fe_2O_3		Classification			
Kangra		68.97		21.62		9.40		[2]Calsialic-LA			
El Cerrejon		84.73		7.97		7.31		[3]Sialic-MA			
		Mineralogy of LTA from coal samples (wt%) based on XRD and SIROQUANT									
		Quartz	Kaolinite	Feldspar (Alb.)	Illite	Calcite	Ankerite	Siderite	Pyrite		
Kangra		15.4	48.9	4.1	<	7.8	4.6	0.9	1.4		
El Cerrejon		34.5	29.7	6.5	21.9	<	<	<	1.4		
			Jarosite	Analcite (?)	Rutile (?)	Bassanite	Anhydrite				
Kangra			2.2	3	2.2	4.1	5.4				
El Cerrejon			2.2	<	<	1.9	1.9				
			Coal trace elements (ppm, dry basis).								
			Cr	Cu	Mn	Ni	Pb	Zn			
Kangra			8.3	12.6	60.3	13.3	9.8	12.8			
El Cerrejon			14.5	9.8	52.4	9.9	<	24.8			
Clarke[4]			12	8	100	8	3	18			
Ranges[5]			0.5–60	0.5–50	5–300	0.5–50	2.–80	5–300			

a.r. –as received; d.b. – dry basis; σ - standard deviation; V - vitrinite; L - liptinite; I - inertinite; MM - mineral matter.

n.d.: not determined; <: Below Quantification Limit.

[1] Mean value for 43 coal ashes worldwide (Vassilev et al., 1995); [2] Calsialic, Low Acid tendency; [3] Sialic, Medium Acid tendency; [4] Clarke for subbituminous coals and coal ashes (Yudovich et al., 1985); [5] Ranges for most coals (Swaine, 1990).

The mineralogy of the Kangra coal LTA is dominated by quartz and kaolinite, with minor proportions of feldspar, calcite, ankerite (or iron-rich dolomite), bassanite, and anhydrite. Pyrite and jarosite (possibly representing an oxidation product of pyrite) are also present, along with a component tentatively identified as analcite. Bassanite and anhydrite probably represent products derived from interaction of organically-associated Ca and organic sulfur during the low-temperature ashing process (Matjie et al., 2008; Pinetown et al., 2007; Ward, 2002). Jarosite was probably formed by oxidation of the pyrite in the coal with exposure and storage (Lopez & Ward, 2008), but may also have been derived from partial oxidation of pyrite during the plasma-ashing process. Although not detected in the XRD analysis, monazite was also found in the Kangra coal using SEM/EDS techniques.

The LTA of the El Cerrejon coal contains more quartz and less kaolinite than that of the Kangra LTA, and has a significant proportion of illite. It contains similar proportions of feldspar, pyrite, and jarosite to the Kanga LTA, but does not contain detectable concentrations of the carbonate minerals (calcite, dolomite/ankerite, or siderite). The LTA of the El Cerrejon sample also has lesser proportions of bassanite and anhydrite than that of the Kangra sample, suggesting a lesser proportion of organically-associated Ca in the El Cerrejon component of the feed coal.

The chemical composition of the HTA for each of the coals reflects the differences in mineralogy. The ash of the Kangra coal contains lesser proportions of SiO_2, K_2O, and Na_2O than the El Cerrejon HTA, but higher proportions of CaO, MgO, and SO_3. This reflects the greater abundance of calcite, ankerite, bassanite, and anhydrite in the LTA of the Kangra coal, and the greater abundance of quartz and illite in the El Cerrejon LTA. Under the classification proposed by Vassilev and Vassileva (2007), the Kangra coal would be categorized as calsialic with a low acid tendency and the El Cerrejon coal as sialic with a medium acid tendency (Table 1; Figure 2).

The trace elements analyzed (Cr, Cu, Mn, Pb, Zn, and Ni) in both coals have values close to the Clarke, and low values in relation to the range for most coals (Swaine, 1990; Yudovich et al., 1985; Table 1).

3.2. Characterization of fly ashes

3.2.1. Fly ash granulometry

The fineness results of the fly ashes (retention on 45-μm sieve, Table 2) show that Economizer and Air-heater fly ashes are coarser than required by Portuguese (Cabaço & Aroso, 1988; Rocha, 1999) and International (Malhotra & Ramezanianpour, 1994) fineness standards for fly ash to be used in concrete production, but the ESP-h12 and ESP-h42 fly ashes have fineness values inside the relevant ranges.

The cumulative distribution of particles at 25 μm, 45 μm, 75 μm, and 150 μm as determined by laser granulometry analysis (Table 2) also shows major variations with sampling location. The cumulative distribution up to 25 μm, for example, shows Economizer <

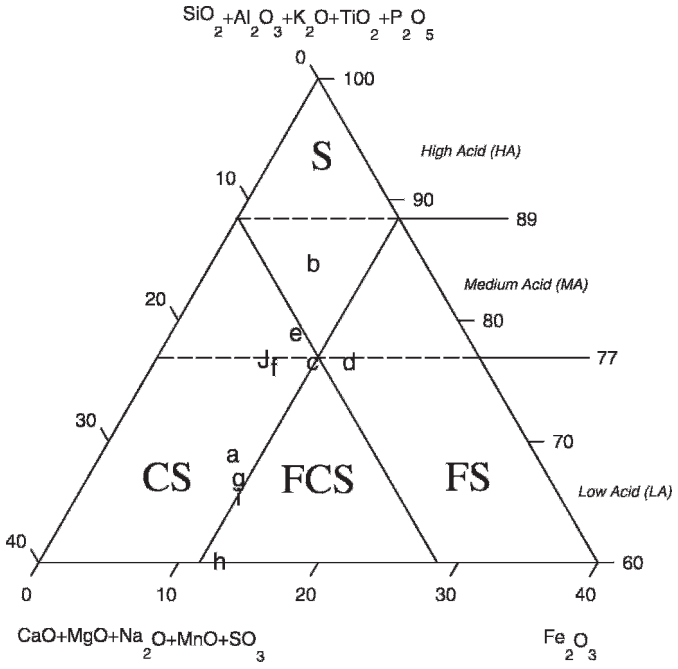

Fig. 2. Chemical classification of coal HTA, FAs, and FA glass. Coals: a) Kangra; b) El Cerrejon. FAs c) Economizer; d) Air-heater, e) ESP-h12; f) ESP-h42. FA glass: g) Economizer; h) Air-heater; i) ESP-h12; J) ESP-h42.
S: Sialic; FS: Ferrisialic; FCS: Ferricalsialic; CS: Calsialic.

Air-heater ≪ ESP-h12 ≪ ESP-h42; in fact the <25-μm values are very high for the ESP-h42 ash sample.

Within different rows this TPP produces fine-grained ash useful for the cement industry and, at the same time, coarse fly ash less suitable for that purpose.

3.2.2. Fly ash chemistry

3.2.2.1. Sulfur and carbon

Sulfur

Total sulfur and SO_3 vary with sampling location in the order Economizer=Air-heater ≪ ESP-h12 < ESP-h42 (Table 2). Since there is a very good positive correlation coefficient (Figure 3) between total sulfur and SO_3, and gypsum and anhydrite were only detected by XRD at ESP-h42, the sulfur trend observed is most probably related with these two dominant S-bearing species in the fly ashes (Vassilev & Vassileva, 1996a, 2007).

Carbon

The total carbon and LOI percentages are very similar for all of the ash samples, except for the Air-heater sample in which the carbon value is very low (Table 2). The low total carbon and LOI percentages in the Air heater sample are most probably due to the gas flow kinetics and the particle aerodynamics and density, as a result of which segregation occurred and the capture of carbonaceous particles by the sampling system was reduced.

The LOI results (Table 2) give values slightly higher than the unburned carbon content; the difference is most probably due to dehydration or decomposition of minerals in the fly ash and also release of volatile organic compounds (Fan & Brown, 2001).

Slight differences in the total carbon and the carbon species contents observed between ESP-h12 and ESP-h42 (Table 2) may be related to the capture of higher proportions of submicron carbon in ESP-h42, since the value of the graphitic carbon increases in the ESP-h42 sample. An HRTEM-STEM-EELS study of fly ash derived from a U.S. bituminous coal has shown the presence of nanoscale (10-s nm) C agglomerates with typical soot-like appearance and others with graphitic fullerene-like nanocarbon structures (Hower et al., 2008).

Table 2
Granulometric and chemical fly ash characterization and classification

Sample location:	Economizer	Air-heater	ESP-h12	ESP-h42
[1]Fineness: retention on a 45-μm sieve (wt%)				
	68	82	22	14
Laser granulometry (cumulative distribution)				
≤25 μm	16.5	17.6	51.6	84.8
≤45 μm	29.7	29.5	69.0	89.6
≤75 μm	47.8	44.7	82.3	93.6
≤150 μm	75.9	73.6	93.8	97.6
Moisture (a.r., wt%)	0.4	0.5	1.3	0.7
Ash (a.r., wt%)	90.8	98.3	89.8	89.4
Ash (d.b., wt%)	91.2	98.8	91.0	90.0
[2]Total Sulfur (%)	0.12	0.11	0.20	0.62
[2]Total carbon (%)	9.24	1.46	8.67	9.27
[2]Organic carbon (%)	7.73	1.19	7.28	7.63
[2]Graphitic carbon (%)	1.23	0.15	1.04	1.48
[2]Inorganic carbon (CO_2; %)	1.02	0.44	1.26	0.60
[2]LOI (%)	10.5	1.6	9.8	11.1
[3]Major oxides and LOI (normalized to 100%), wt%				
SiO_2	49.08	56.96	45.91	41.99
Al_2O_3	19.20	16.48	23.50	23.15
K_2O	0.77	0.67	0.79	0.90
Ti_2O	0.94	0.93	1.11	1.32
P_2O_5	0.35	0.31	0.51	1.30
Na_2O	0.27	0.24	0.34	0.34
CaO	8.52	6.95	8.09	8.69
MgO	1.98	1.80	1.98	2.67
MnO	0.06	0.07	0.05	0.07
Fe_2O_3	10.42	13.69	8.09	7.89
SO_3	0.25	0.26	0.57	1.89
LOI	8.16	1.65	9.04	9.81
Total	100.02	100.00	99.99	100.01
[4]Basicity modulus (after normalization to 100%)				
M_b ($CaO+MgO/SiO_2+Al_2O_3$)	0.15	0.12	0.15	0.17
[5]Chemical classification (values normalized to 100%)				
	$SiO_2+Al_2O_3+K_2O+TiO_2+P_2O_5$	$CaO+MgO+SO_3+Na_2O+MnO$	Fe_2O_3	Classification
Economizer	76.6	12.1	11.3	Calsialic, Low acid
Air-heater	76.6	9.5	13.9	Ferrisialic, Low acid
ESP-h12	79.0	12.1	8.9	Calsialic, Medium acid
ESP-h42	76.1	15.1	8.7	Calsialic, Low acid

[1] NP EN 451-2 1995 [ISO 565].

[2] Total carbon and total sulphur (Leco method), carbon species, inorganic carbon (CO_2) and LOI (1000°C) were conducted at ACME Analytical Laboratories, LTD.

[3] Determined at University of New South Wales.

[4] Basicity modulus according to Anshits et al. (2001).

[5] Chemical classification according to Vassilev and Vassileva (2007).

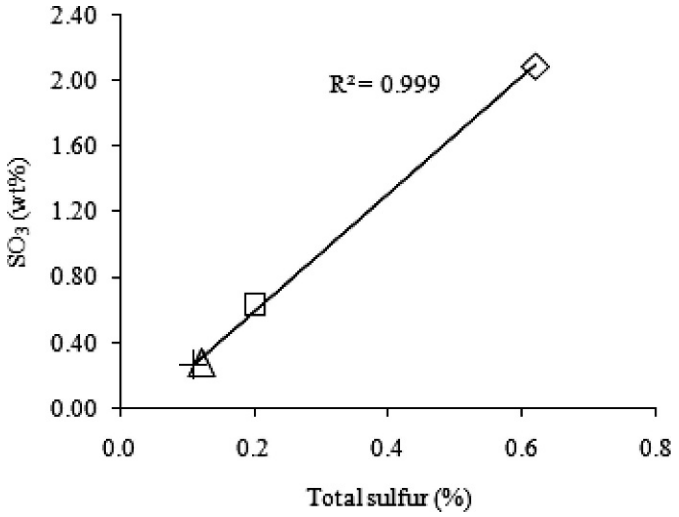

Fig. 3. Correlation between total sulfur and SO_3 determined for fly ashes from the different sampling locations. Economizer (△); Air-heater (+); ESP-h12 (□); ESP-h42 (◇).

The variations in the percentage of inorganic carbon (CO_2) (Table 2) are probably related to the presence of Ca carbonates in the coal ashes. The highest percentages of CO_2 are found in the Economizer and ESP-h12 samples, XRD analysis of which (Table 2) indicates significant proportions of calcite. Calcite was not identified by the XRD study in the Air-heater and in the ESP-h42 samples, where the CO_2 percentages are the lowest; it may have been present but below the detection limit. Calcite in feed coal would be expected to decompose at the temperatures inside the combustion chamber, and hence, as suggested by Bauer and Natusch (1981), the presence of calcite in the ashes may reflect interaction of Ca or CaO with CO_2 in the furnace atmosphere further down the combustion stream. Bauer and Natusch (1981) indicate that calcite may form in fly ash by interaction of CaO and CO_2 at temperatures between ~400 °C and the decomposition temperature of calcite (around 800 °C), and this may explain its occurrence in the Economizer sample of the present study. Bauer and Natusch (1981) suggest that calcite may also form at lower temperatures, aided by the presence of water vapor, such as during cooling of ash after it has been captured by precipitators. Temperature differences, density factors and/or particle aerodynamics may be responsible for the absence of calcite from the Air-heater sample in the present study, but the presence of calcite in the ESP-h12 sample may represent lower-temperature CO_2 take-up, either in the ash stream or during cooling in the ash hopper after capture.

3.2.2.2. Chemical classification

Chemical classification of coal HTA and bulk FAs

The coal HTA and the fly ash chemical classification (Tables 1 and 2) are both based on the major oxides involved (Roy & Griffin, 1982; Vassilev & Vassileva, 2007). Although the resulting fly ashes plot between the HTAs of the individual coals blended to constitute the feed, none of the FAs has the same chemical classification (Figure 2). Variations in alkaline and Fe oxides result in variations in the chemical classification of the individual ash samples. In the ESP, the variations found are due to the Fe_2O_3 content, which is probably related to the magnetic and electrostatic properties.

Table 3
XRD characterization of the fly ashes and inferred glass composition and classification

Sample location:	Economizer	Air-heater	ESP-h12	ESP-h42
X-ray diffraction analysis results from ZnO spiked fly ash Samples				
Phase	wg %	wg %	wg %	wg %
Quartz	12.7	25	9.1	3.8
Mullite	16.6	15.2	19.9	11
Magnetite	3	2.6	2.5	0.8
Maghemite	2.2	2.6	1.2	1.3
Hematite	1.4	2	1.4	0.9
Anorthite	2.9	7.1	<	<
Calcite	0.6	<	1.2	<
Diopside (?)	<	1.2	<	<
Anhydrite	<	<	<	2.6
Gypsum	<	<	<	1.4
Amorphous (glass)	60.6	44.4	64.7	78.2
[1]Phase-mineral classification system				
Glass	60.6	44.4	64.7	78.2
Quartz+ mullite	29.3	40.2	29	14.8
[2]Active	10.1	15.5	6.3	7
Classification	[3]Inert-LP	[3]Inert-LP	[4]Inert-LMP	[5]Pozzolanic-HP
Inferred chemistry of the fly ash glass				
SiO_2	40.77	30.87	47.1	51.39
Ti_2O	2.13	3.17	1.98	1.64
Al_2O_3	19.83	20.98	12.53	20.95
Fe_2O_3	10.61	12.69	11.48	7.65
MgO	4.6	5.6	4.42	3.53
CaO	15.06	18.01	15.28	11.05
Na_2O	1.97	2.71	1.83	1.51
K_2O	1.97	2.49	1.52	1.39
P_2O_5	1.48	2.03	1.52	1.14
SO_3	0.33	0.45	1.22	−0.64
H_2O	<	<	<	0.38
CO_2	1.24	0.99	1.11	<
Total	100	100	100	100
[4]Basicity modulus: M_b ($CaO+MgO/SiO_2+Al_2O_3$)				
	0.32	0.46	0.33	0.20
[5]Chemical classification based on inferred chemistry				
	$SiO_2+Al_2O_3$ $+K_2O+TiO_2$ $+P_2O_5$	$CaO+MgO$ $+SO_3$ $+Na_2O$	Fe_2O_3	Classification
Economizer	67.0	22.2	10.7	Calsialic, Low acid
Air-heater	60.1	27.0	12.8	Ferricalsialic, Low acid
ESP-h12	65.4	23.0	11.6	Calsiali-Ferricalsialic, Low acid
ESP-h42	76.8	15.5	7.7	Calsialic, Low-medium acid

<: not present or below the limit of detection of the XRD system; [1] According with Vassilev and Vassileva (2007); [2] Active: Oxyhydroxides+Sulphates+Carbonates+Other silicates; [3] Inert low pozzolanic; [4] Inert Low-Medium pozzolanic; [5]Pozzolanic high pozzolanic.

Chemical classification of the FA glass

For comparative purposes, the same parameters based on the inferred chemistry of the FA glass fractions (Table 3) were also plotted on the same ternary diagram (Figure 2) as the bulk FA chemical analyses. In this case, the inferred chemical composition of the glass in the Economizer, Air-heater, and ESP-h12 samples is more alkaline than the bulk composition of the respective bulk FAs and the acidity tendency is, therefore, lower. All of these glasses have a similar composition and are classified near the Kangra coal. It is possible that Ca in carbonates and organically-bound Ca in both coals were mobilized due to the high temperature conditions and joined Si-Al melts which produced the massive-microporous glassy microspheres. By contrast, more acid (Si-rich) melts led to

the small size microporous-cenospheric glassy morphotypes abundantly present in the sample from ESP-h42.

The proportion of glass found in the sample from ESP-h42 is much higher than in the other samples (Table 3) although the chemical composition and classification of the bulk FA and the glass are similar.

3.2.3. Mineralogy

Table 3 provides a summary of the estimated weight percentages of the phases recognized in each ash by XRD analysis of the ZnO-spiked samples.

Amorphous material (or glass) is the main inorganic component of the fly ashes studied. The proportion of amorphous material (glass) in the ash from each hopper increases downstream through the ash collection system. The glass was probably derived from melting and recrystallisation of residues from thermal decomposition of the minerals and non-mineral inorganics in the feed coal at the high temperatures of the combustion chamber (Matjie et al., 2008).and may present a wide range of sizes, density, and compositions that influence capture by collection systems.

The ash from each location has different proportions of the various mineral and amorphous components; for example the ash from the upstream sampling locations (Economizer and Air-heater) have higher proportions of quartz, possibly derived from quartz in the feed coal preserved due to the high melting temperature of this mineral (Hower et al., 1997; Querol et al., 1994) combined with the lower combustion temperatures associated with low-NO_x burners (Robl et al., 1995). SEM/EDS observations indicate that the quartz typically occurs as very large grains, probably originally of detrital origin, especially at the locations closest to the furnace, or inside small glassy fly ash spheres. Quartz skeletons (Hulett & Weinberger, 1980) forming part of microspheres, which cannot be identified unless etching is used, may be partially responsible for the occurrence of quartz in the more downstream samples such as ESP-h42.

Anorthite seems to be confined to the ashes from the economizer and air heater (Table 3), and anhydrite/gypsum to the last part of the precipitator section (ESP-h42).

Anorthite was not observed during the SEM study, so that textural data are not available to resolve whether the mineral represents remnants of detrital feldspar grains in the coal (angular fragments), or whether it represents feldspar produced by either solid-state reactions or crystallisation from melting (euhedral crystals) in the course of ash formation. Experience elsewhere suggests that the anorthite in coal ash is a product of reactions between Ca and aluminosilicate residues of the clay minerals in the high-temperature part of the combustion system (Matjie et al., 2008), and therefore the occurrence of feldspar only in the samples from close to the furnace might suggest high-temperature formation, possibly associated with incipient slag droplets.

Anhydrite was probably formed by conversion of calcite or organically-associated Ca to lime, followed by reaction with SO_2 in the combustion stream (Koukuzas et al., 2007), while the gypsum is probably a tertiary mineral resulting from hydration of anhydrite during storage and sampling preparation (Vassilev & Vassileva, 1995, 1996a).

Mullite is thought to have mainly originated by solid-state reaction of kaolinite and other clay minerals, and is typically incorporated into the glassy matrix of ash spheres (Hulett & Weinberger, 1980). Mullite occurs in the ash from all of the sampling locations.

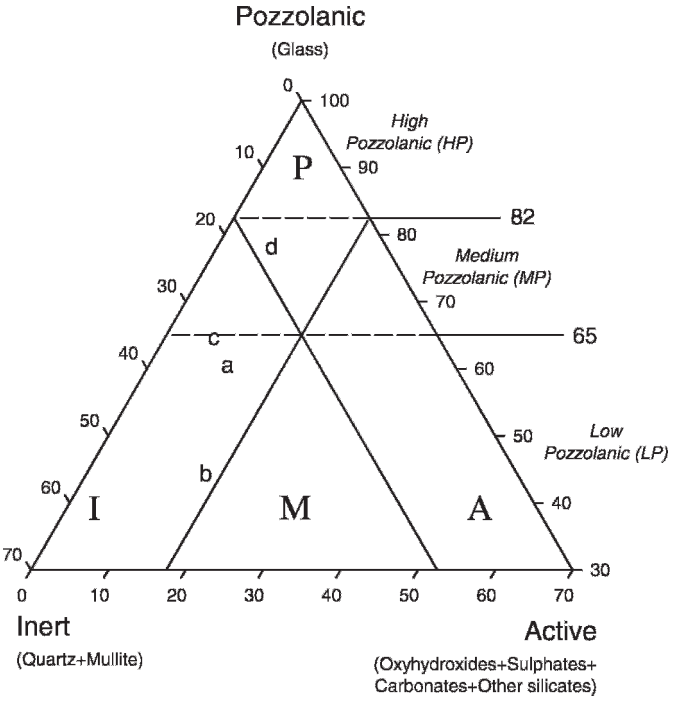

Fig. 4. Phase-mineral classification of fly ashes from four sampling locations inside a power plant: a) Economizer; b) Air-heater; c) ESP-h12; d) ESP-h42. Abbreviations for phase-mineral fly ashes type are: P (Pozzolanic); I(Inert); M (Mixed); A (Active).

The Fe-oxides, magnetite and hematite, probably resulted from oxidation of pyrite and other Fe-bearing minerals (e.g. siderite), whereas maghemite may be an oxidation product of magnetite. All these Fe minerals occur, in most cases, embedded in a Fe-rich aluminosilicate glass and are the main components of ferrospheres (Lauf et al., 1982; Anshits et al., 1998). Therefore, density and magnetic properties (Anshits et al., 2000) may be responsible for capture and segregation at the sampling locations.

Phase-mineral classification

The phase-mineral fly ash classification system proposed by Vassilev and Vassileva (2007) was used to classify our fly ashes (Table 3; Figure 4), and to show in another way the variation with each sampling location. By making an analogy to natural geologic systems, it seems that each location inside the TPP has the ability to produce its own ''rock'' composition, either due to density and aerodynamics of the particles in the gas flow or due to collecting systems conditions. An understanding of these variations may be useful to allow production of fly ash fractions with specific properties from the TPP instead of only a composite fly ash.

3.2.4. Morphology

SEM/EDS of bulk samples

Studies of the different samples with SEM/EDS (Figure 5) also show that the ash from each sampling location has its own composition and particle distribution, although some morphotypes (char and char fragments, large- and micro- glassy spheres, glassy agglomerations, and iron-rich spheres) are present, in different proportions, in the samples from all locations.

Relatively high proportions of large particles are found in those samples from locations nearest to the furnace. These are composed

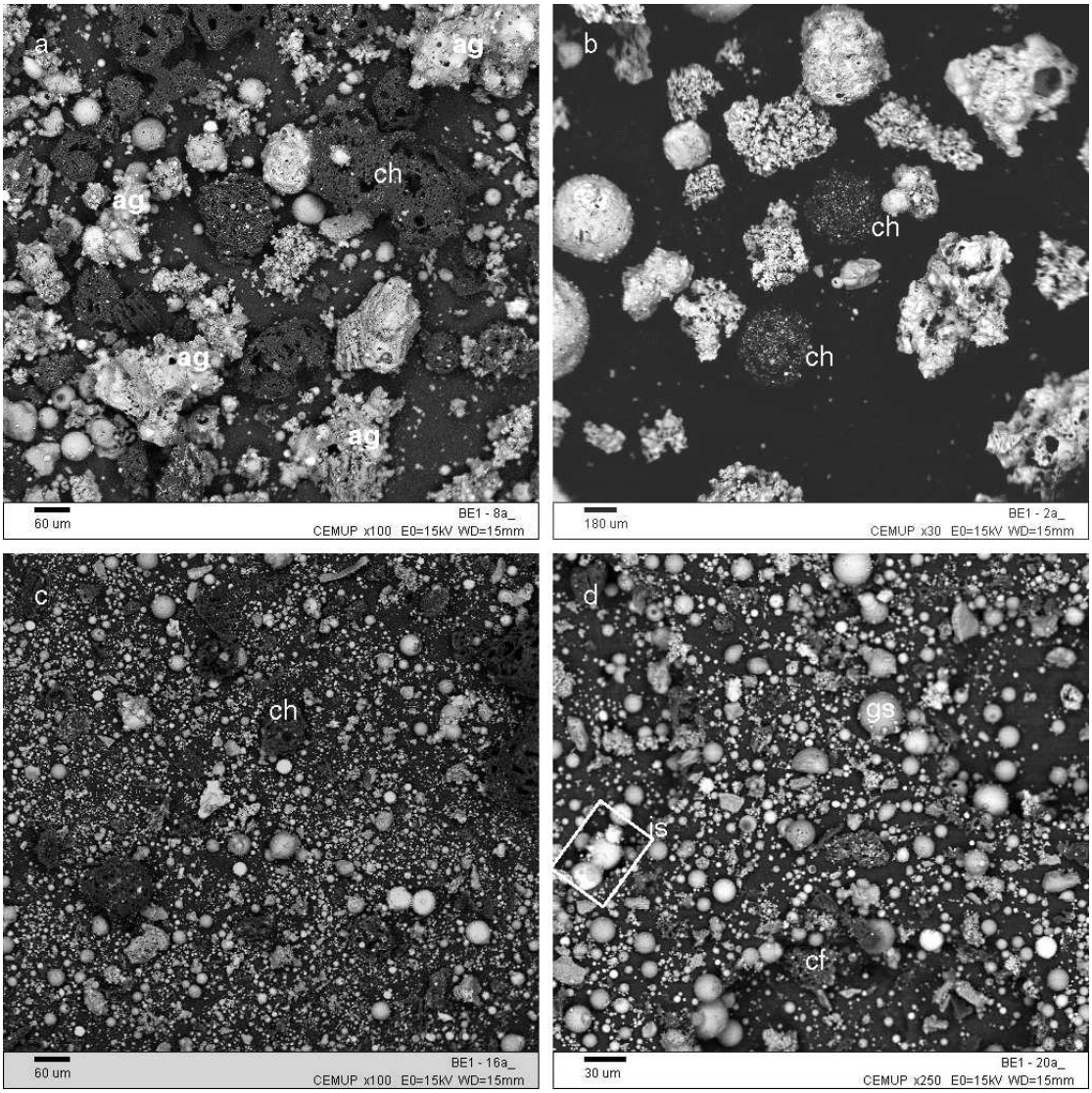

Fig. 5. SEM overview of the different sampling locations: a) Economizer: large particles of char (ch) and agglomerations (ag); b) Air-heater: most particles are large with irregular shape, and char is minor component; c) ESP h12: large char particles, smaller glass spheres and iron-spheres, and a background of micro-glassy-spheres; d) ESP h42: char fragments (cf), glassy spheres (gs) and iron-spheres (is), in a background of micro-glassy-spheres.

of char, glassy agglomerates, and minerals (especially quartz), and most probably formed due to density segregations inside the flow. Much smaller particles are found in the ESP hoppers. Some heterogeneity in these particles can be seen in the sample from ESP-h12. The ash from ESP-h42 is more homogeneous consisting mainly of micrometer-sized glassy spheres.

The upstream end of the ESP system collects the most (about 80%) and collects the coarsest ash (Hower et al., 2001; Mardon and Hower, 2004). At the downstream end the smallest and least conductive particles are captured, but even so around 0.2% of the particles are released to the atmospheres through the stack (Figure 6). These consist of glassy micrometer and sub-micrometer (1–10 μm and $<$ 1 μm) spheres with different compositions, particles (0.1–1 μm) attached to the surface of the larger spheres, and char.

SEM images of fly ash obtained this way could be used to describe the type of microspheres; however, only the surface composition and morphology can be assessed using SEM techniques. There seems to be a trend from more irregular particles (such as glassy agglomerates) in the Economizer and Air-heater hoppers up to smooth and spherical particles at the end of the ash collection stream (ESP-h42).

ESEM/EDS of FA polished blocks and Basicity modulus

Since different morphology types of microspheres may be derived from melts of different composition, the Basicity modulus [M_b=(CaO+MgO)/(SiO_2+Al_2O_3)] was used by Anshits et al. (2001) to classify glass morphotypes, with key values for the ratio being 0.8 for massive microspheres and 0.2 for porous microspheres. Cenospheres (thin-walled porous glass) are characterized by the lowest Basicity modulus, equal to 0.05.

Calculation of the Basicity modulus based on the major oxide results derived from bulk FA samples, however, does not represent only that of the FA glass.

Considerations about FA structure using major oxide analyses and SEM micrographs do not match. Although essentially glassy

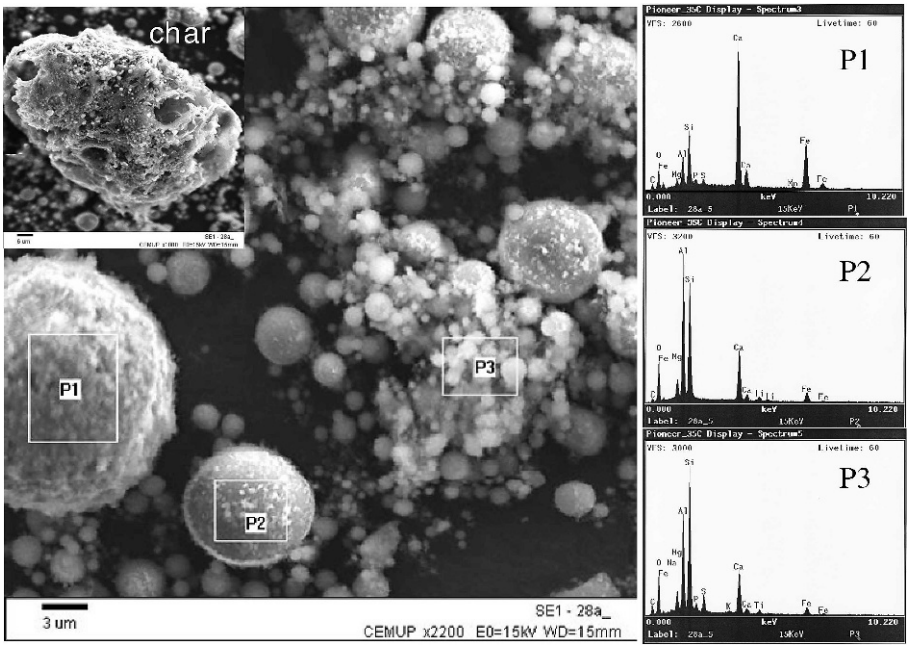

Fig. 6. SEM/EDS of stack FA.

porous microspheres and cenospheres would be expected (Table 2), analysis of FA cross sections in polished blocks using an ESEM in backscattered mode (Figure 7) shows mostly massive microspheres and very few cenospheres. Valentim et al. (2009) have already verified that the light fraction (1g/cm^3; characterized by the abundance of glassy cenospheres) of the Economizer FA comprised less than 2% of the total sample, meaning that glassy cenospheres could not be abundant.

Once it was possible to infer the composition of the glass in the FAs (Table 3), the Basicity modulus of the glass fraction was determined for each sample using the inferred oxide percentages. The Basicity modulus results obtained in this way are in closer agreement with the ESEM observations and the sink-float results, suggesting a shift to the massive morphology side instead to the cenospheric side.

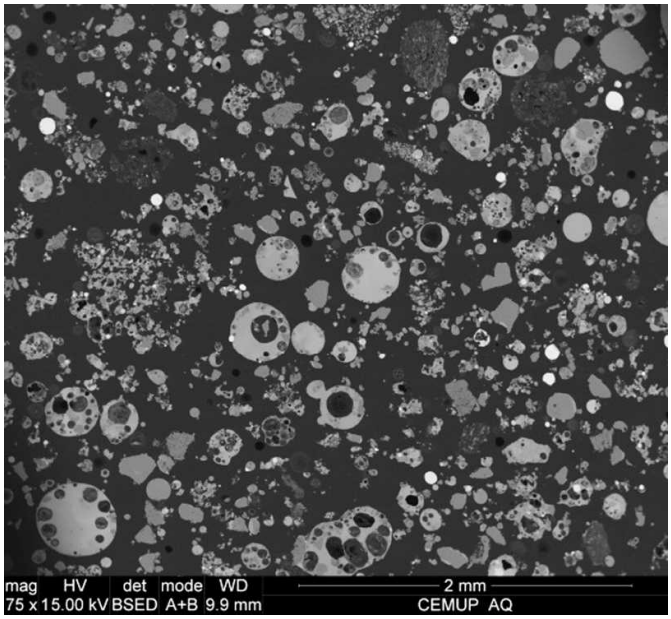

Fig. 7. Cross section polished block of FA from the Air-heater (ESEM backscattered mode).

3.2.4. Trace elements and relative enrichment factors (REs)

Six trace elements (Cr, Cu, Mn, Ni, Pb, and Zn) considered to be of environmental interest (Swaine, 2000) were chosen to evaluate variations in trace elements concentration with sampling location. The results from this study were also compared with the ranges of trace elements reported in the literature for fly ashes from other countries (Table 4).

The relative enrichment factors (REs) of these elements was also calculated through the Meij factor (Meij, 1994), as follows (equation 1):

$$\mathrm{RE} = (\textit{conc. in ash}/\textit{conc. in coal}) \times (\%\ \textit{ash content in coal}/100) \quad (1)$$

The results of these determinations are listed in Table 4 and illustrated in Figure 8.

All these elements were classified as Class II by Meij (1994), with the suggestion that they will be vaporized in the boiler and that complete condensation will occur within the ash collection system on the surface of the fly ash particles (RE will be ≈1 for ESP fly ashes). However, the behaviour of the individual elements is different, and hence they were also subdivided by the expected order of volatilization: Mn and Cr (Class IIc) < Ni and Cu (Class IIb) < Pb and Zn (Class IIa) (Meij, 1994).

In general, the concentrations of these trace elements in the ashes (except Mn) increase down the flow path in the order Economizer= Air-heater < ESPh12 < ESP-h42. This trend may in part be related to decreasing temperature, decreasing particle size (ESP-h42 has the largest proportion of particles <25-μm), and changes in element volatility. The relative enrichment (RE values) of the trace elements studied (except Mn) also shows variation with the sampling location (Figure 8), with the fly ashes from the Economizer to ESP-h42 being progressively enriched in Cr, Cu, Ni, Pb, and Zn.

Table 4 also shows the range of trace element concentrations reported for other coal ashes, as a basis for comparison to the

Table 4
Trace elements (Cr, Cu, Mn, Ni, Pb, and Zn) in fly ashes from four sampling locations, relative enrichment factors (Meij, 1994), and international fly ash reports

Sample location:	Economizer	Air-heater	ESP-h12	ESP-h42
Trace elements (ppm, dry basis).				
Cr	99.5	101.6	137.9	180.1
Cu	38.0	34.9	51.2	74.1
Mn	452.5	541.8	399.6	470.4
Ni	67.2	62.8	77.5	104.4
Pb	13.9	9.6	37.2	65.3
Zn	30.1	36.6	63.9	182.4
[1]Relative enrichment factor (RE), after Meij (1994).				
	Economizer	Air-heater	ESP-h12	ESP-h42
Cr	1.1	1.1	1.5	2.0
Cu	0.4	0.4	0.6	0.8
Mn	1.0	1.2	0.9	1.1
Ni	0.7	0.7	0.8	1.1
Pb	0.4	0.2	1.0	1.7
Zn	0.2	0.2	0.4	1.2
	Results from other authors			
	[2]Aust. and US coals fly ash		[3]Bituminous coals fly ash	
Trace elements (ppm)	Mean	RE	Range	RE range
Cr	131	1	101.5–176	0.62–0.88
Cu	151	1	123.5–151	0.75–0.94
Mn	415	1	774.4–1168	0.46–1.11
Ni	98	1	105.6–135	0.69–0.87
Pb	77	1	61.5–79	0.07–0.96
Zn	218	1	98.2–140	0.71–1.39
	[4]Subbituminous coals fly ash		[5]West. U.S. coals fly ash	[6]India coals fly ash
Trace elements (ppm)	Study 1–2	RE	Mean	Mean
Cr	103–52	1.20–1.00	54	120
Cu	66.1–53	0.98–1.20	63	100
Mn	366–350	0.99–0.90	200	339
Ni	33.5–34.1	0.82–1.20	34	150
Pb	64.3–84.2	1.64–1.60	48	35
Zn	126–155	1.70–1.60	72	[7]60–124

[1] Ash (d.b.) of the feed is a mean value since it is composed by a 50:50 blend of two coalsn; [2] Meij (1994); [3] Danihelka et al. (2003); [4] Goodarzi (2006); [5] Valkovic (1983); [6] Sivakumar and Datta (1996); [7] Sushil et al. (2006).

results of the present study. Since the feed coals and combustion conditions represented by those samples are all different and since we did not study composite fly ash samples as part of the present study, comparing our trace element concentrations with those reported elsewhere is of limited value. However, it can be seen that the concentrations of the trace elements, and the associated REs, are somewhat different to the previously published results. Similar concentrations and REs in relation to global averages are noted in the present study for Mn and Cr; this may reflect the low volatility of these elements. The most marked differences are shown by Cu, Pb, Ni and Zn; these could be related to variations in particle size and temperature, especially in the Economizer/Air-heater and ESP-h42 samples, compared to the composite samples reported in other studies.

5. Conclusions

The fly ash captured inside a TPP may vary in character from one location to another, due to changes in furnace conditions and the type of collecting system. Collection points nearest to the furnace appear to have the coarsest FA particles, and are also richer in large-size char and in residual minerals from the feed coal, such as detrital quartz, if the original grains were large enough.

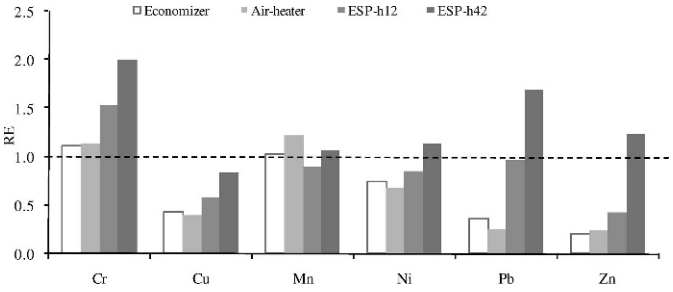

Fig. 8. Relative Enrichment factors (RE) of Cr, Cu, Mn, Ni, Pb and Zn from four different sampling locations.

The electrostatic properties of the particles are crucial for collection by ESPs, and the upstream end of such systems is able to capture very different types of particles to the downstream end. At the output end of the precipitator, only the smallest and most inert particles appear to be captured.

The temperature decrease from the furnace to the stack also contributes to variations in fly ash composition inside the TPP, due in part to condensation of trace elements. In the present study the concentration of elements such as Cr, Pb, Zn, Cu, and Ni increased towards the cooler end of the collection system.

Acknowledgements

The authors thank the Fundação para a Ciência e a Tecnologia (Portugal) and FEDER (UE) for financing the Project, Contract POCTI/CTA/38997/01.

References

Anshits, A.G., Kondratenko, E.V., Fomenko, E.V., Kovalev, A.M., Anshits, N.N., Bajukov, O.A., Sokol, E.V., Salanov, A.N., 2001. Novel glass crystal catalysts for the processes of methane oxidation. Catalysis Today 64, 59–67.

Anshits, A.G., Kondratenko, E.V., Fomenko, E.V., Kovalev, A.M., Bajukov, O.A., Sokol, E.V., Anshits, N.N., Kochubey, D.I., Boronin, A.I., Salanov, A.N., Koshcheev, S.V., 2000. Physicochemical and catalytic properties of glass crystal catalysts for the oxidation of methane. Journal of Molecular Catalysis A: Chemical 158, 209–214.

Anshits, A.G., Voskresenskaya, E.N., Kondratenko, E.V., Fomenko, E.V., Sokol, E.V., 1998. The study of composition of novel high temperature catalysts for oxidative conversion of methane. Catalysis Today 42, 197–203.

ASTM D3172, 2007a, Standard Practice for Proximate Analysis of Coal and Coke. ASTM International, West Conshohocken, PA, www.astm.org.

ASTM D3682 – 01, 2006, Standard Test Method for Major and Minor Elements in Combustion Residues from Coal Utilization Processes. ASTM International, West Conshohocken, PA, www.astm.org.

Bailey, J.G., Tate, A., Diessel, C.F.K., Wall, T.F., 1990. A char morphology system with applications to coal combustion. Fuel 69, 225–239.

Bauer, C.F., Natusch, D.F.S., 1981. Identification and quantitation of carbonate compounds in coal fly ash. Environmental Science and Technology 15, 783–88.

Block, C., Dams, R., 1976. Study of fly ash emission during combustion of coal. Environmental Science and Technology 10, 1011–1017.

Cabaço, R., Aroso, M.E., 1988. Utilização das cinzas volantes da central termoeléctrica de Sines em betões e argamassas de cimento. Congresso da Ordem dos Engenheiros 1988, pp. 1–20 (in Portuguese).

Clarke, L.B., 1993. The fate of trace elements during coal combustion and gasification: an overview. Fuel 72, 731.736.

Conzemius, R.J., Welcomer, T.D., Svec, H.J., 1984. Elemental partitioning in ash depositories and material balance for a coal burning facility by spark source mass spectrometry. Environmental Science and Technology 18, 12–18.

Danihelka, P., Volna, Z., Jones, J.M., Williams, A., 2003. Emissions of trace toxic metals during pulverized fuel combustion of Czech coals. International Journal of Energy Research 27, 1181–1203.

Donahoe, R.J., Bhattacharyya, S., Patel, D., Ladwig, K.J., 2007. Chemical fixation of trace elements in coal fly ash. World of Coal Ash (WOCA), May 7–10, 2007, Covington, Kentucky, USA.

Fan, M., Brown, R. C., 2001. Comparison of the Loss-on-Ignition and Thermogravimetric Analysis Techniques in Measuring Unburned Carbon in Coal Fly Ash. Energy & Fuels 15, 1414–1417.

Finkelman, R.B., Palmer, C.A., Krasnow, M.R., Aruscavage, P.J., Sellers, G.A., Dulong, F.T., 1990. Combustion and leaching behavior of elements in the Argonne Premium Coal Samples. Energy & Fuels 4, 755–766.

Fomenko, E.V., Kondratenko, E.V., Salanov, A.N., Bajukov, O.A., Talyshev, A.A., Maksimov, N.G., Nizov, V.A., Anshits, A.G., 1998a. Novel microdesign of oxidation catalysts. Part 1. Glass crystal microspheres as new catalysts for the oxidative conversion of methane. Catalysis Today 42, 267–272.

Fomenko, E.V., Kondratenko, E.V., Sharonova, O.M., Plekhanov, V.P., Koshcheev, S.V., Boronin, A.I., Salanov, A.N., Bajukov, O.A., Anshits, A.G., 1998b. Novel microdesign of oxidation catalysts. Part 2. The influence of fluorination on the catalytic properties of glass crystal microspheres. Catalysis Today 42, 273–277.

French, D., Riley, K., Ward, C.R., 2007. Characterisation, classification and properties of coal combustion products. Coal Combustion Products Handbook, (Gurba, L.W., Heidrich, C. and Ward, C.R., eds), Co-operative Research Centre for Coal in Sustainable Development, Brisbane, pp. 37–100.

Goodarzi, F., 2006. Characteristics and composition of fly ash from Canadian coal-fired power plants. Fuel 85, 1418–1427.

Hansen, L.D., Silberman, D., Fisher, G.L., 1981. Crystalline components of stack-collected, size-fractionated coal fly ash. Environmental Science and Technology 15, 1057–1062.

Haynes, B., Neville, M., Quann, R.J., Sarofim, A.F., 1982. Factors governing the surface enrichment of fly ash in volatile trace species. Journal of Colloid and Interface Science 87, 266–278.

Hower, J.C., Finkelman, R.B., Rathbone, R.F., Goodman, J., 2000. Intra- and inter-unit variation in fly ash petrography and mercury adsorption: examples from a western Kentucky power station. Energy & Fuels 14, 212–216.

Hower, J.C., Graham, U.M., Dozier, A., Tseng, M.T., Khatri, R.A., 2008. Association of the Sites of Heavy Metals with Nanoscale Carbon in a Kentucky Electrostatic Precipitator Fly Ash. Environmental Science and Technology 42, 8471–8477.

Hower, J.C., Mastalerz, M., 2001. An approach toward a combined scheme for the petrographic classification of fly ash. Energy & Fuels 15, 1319–1321.

Hower, J.C., Rathbone, R.F., Robl, T.L, Thomas, G.A., Haeberlin, B.O., Trimble, A.S., 1997. Case study of the conversion of tangential- and wall-fired units to low-NOx combustion: impact on fly ash quality. Waste Management 17, 219–229.

Hower, J.C., Sakulpitakphon, T., Trimble, A.S., Thomas, G.A., Schram, W.H., 2006. Major and minor element distribution in fly ash from a coal-fired utility boiler in Kentucky. Energy Sources, Part A 28, 79–95.

Hower, J.C., Suarez-Ruiz, I., Mastalerz, M., 2005. An Approach Toward a Combined Scheme for the Petrographic Classification of Fly Ash: Revision and Clarification. Energy and Fuels 19, 653–655.

Hower, J.C., Trimble, A.S., Eble, C.F., 2001. Temporal and spatial variations in fly ash quality. Fuel Processing Technology, 73: 37–58.

Huang, Y., Jin, B., Zhong, Z., Xiao, R., Tang, Z., Ren, H., 2004. Trace elements (Mn, Cr, Pb, Se, Zn, Cd and Hg) in emissions from a pulverized coal boiler. Fuel Processing Technology 86, 23–32.

Hulett, L.D., Weinberger, A.J., 1980. Some etching studies of the microstructure and composition of large aluminosilicate particles in fly ash from coal-burning power plants. Environmental Science and Technology 14, 965–970.

ISO 564, 1990, ''Test sieves - Metal wire cloth, perforated metal plate and electroformed sheet - Nominal sizes of openings,'' International Organization for Standardization, www.iso.org.

ISO 7404-3, 1994, ''Methods for the petrographic analysis of bituminous coal and anthracite – Part 3: Method of determining maceral group composition,'' International Organization for Standardization, www.iso.org.

ISO 7404-5, 1994, ''Methods for the petrographic analysis of bituminous coal and anthracite – Part 5: Method of determining microscopically the reflectance of vitrinite,'' International Organization for Standardization, www.iso.org.

Kaakinen, J.W., Jorden, R.M, Lawasani, M.H.,West, R.E., 1975. Trace element behavior in coal-fired power plant. Environmental Science and Technology 9, 862–869.

Klein, D.H., Andren, A.W., Carter, J.A., Emery, J.F., Feldman, C., Fulkerson, W., Lyon, W.S., Ogle, J.C., Talmi, Y., 1975. Pathways of thirty-seven trace elements through coal-fired power plant. Environmental Science and Technology 9, 973–979.

Koukouzas, N., Hämäläinen, J., Papanikolaou, D., Tourunen, A., Jäntti, T., 2007. Mineralogical and elemental composition of fly ash from pilot scale fluidised bed combustion of lignite, bituminous coal, wood chips and their blends. Fuel 86, 2186–2193.

Laskowski, J.S., 2001. Developments in mineral processing. D.W. Fuerstenau (adv. editor), Elsevier, vol. 14, 368 pp.

Lauf, R.J., Harris, L.A., Rawlston, S.S., 1982. Pyrite framboids as the source of magnetite spheres in fly ash. Environmental Science and Technology 16, 218–22.

López, I.C., Ward, C.R., 2008. Composition and mode of occurrence of mineral matter in some Colombian coals. International Journal of Coal Geology 73, 3–18.

Malhotra, V.M., Ramezanianpour, A.A., 1994. Fly ash in concrete - 2nd edition, CANMET – Canada Centre for Mineral and energy Technology, pp. 307.

Mardon, S.M., Hower, J.C., 2004. Impact of coal properties on coal combustion by-product quality: examples from a Kentucky power plant. International Journal of Coal Geology, 59: 153–169.

Mastalerz, M., Hower, J.C., Drobniak, A., Mardon, S.M., Lis, G., 2004. From in-situ coal to fly ash: a study of coal mines and power plants from Indiana. International Journal of Coal Geology 59, 171–192.

Matjie, R.H., Li, Z., Ward, C.R., French, D., 2008. Chemical composition of glass and crystalline phases in coarse coal gasification ash. Fuel 87, 857–869.

Meij, R., 1994. Trace element behaviour in coal-fired power plants. Fuel Processing Technology 39, 199–217.

Meij, R., Winkel, B.H., 2009. Trace elements in world steam coal and their behaviour in Dutch coal-fired power stations: A review. International Journal of Coal Geology 77, 289–293.

Norrish, K., Hutton, J.T., 1969. An accurate X-ray spectrographic method for the analysis of a wide range of geological samples. Geochimica et Cosmochimica Acta 33, 431–453.

NP EN 451-2, 1994 PT, 1996, ''Portuguese version of the European Standard EN 451-2, 1994,'' ''Method for testing fly ash – Part 2: Determination of fineness by wet sieving,'' Instituto Português da Qualidade (IPQ), Lisboa (in Portuguese).

Pinetown, K.L., Ward, C.R., and van der Westhuizen, W.A., 2007. Quantitative evaluation of minerals in coal deposits in the Witbank and Highveld Coalfields and the potential impact on acid mine drainage. International Journal of Coal Geology 70, 166–183.

Querol, X., Turiel, J.L.F., Soler, A.L., 1994. The behaviour of mineral matter during combustion of Spanish subbituminous and brown coals. Mineralogical Magazine 59, 119.

Raask, E. Mineral Impurities in Coal Combustion. Hemisphere: Washington, DC, 1985.

Rietveld, H.M., 1969. A profile refinement method for nuclear and magnetic structures. Journal of Applied Crystallography 2, 65–71.

Robl, T.L., Hower, J.C., Graham, U.M., Groppo, J.G., Rathbone, R.F., Taulbee, D.N., Medina, S.S., 1995. The impact of conversion to low-NOx burners on ash characteristics.. Am. Soc. Mech. Eng. Oct. 1995, Minneapolis, Mn.

Pinetown, K.L., Ward, C.R., van der Westhuizen, W.A., 2007. Quantitative evaluation of minerals in coal deposits in the Witbank and Highveld Coalfields, and the potential impact on acid mine drainage. International Journal of Coal Geology 70, 166–183.

Rocha, P., 1999. Betões de elevado desempenho com recurso a materiais e processos correntes. Universidade do Minho, Master thesis, pp. 202 (in Portuguese).

Roy, W.R., Griffin, R.A., 1982, A proposed classification system for coal fly ash in mustidisciplinary research. Journal of Environment Quality 11, 563–568.

Senior, C.L., Johnson, S., 2005. Impact of Carbon-in-Ash on Mercury Removal across Particulate Control Devices in Coal-Fired Power Plants. Energy & Fuels 19, 859–863.

Sivakumar, D.S., Datta, M., 1996. Assessment of groundwater contamination potential around ash ponds through field sampling: a review. Ash ponds and ash disposal systems, (Raju VS, ed.). New Delhi, Narosa Publishing House, pp. 311–25.

Sokol, E.V., Kalugin, V.M., Nigmatulina, E.N., Volkova, N.I., Frenkel, A.E., Maksimova, N.V., 2002. Ferrospheres from fly ashes of Chelyabinsk coals: Chemical composition, morphology and formation conditions. Fuel 81, 867–876.

Suarez-Ruiz, I., Valentim, B., 2007. Fly ash components: A proposal for their identification and classification. World of Coal Ash (WOCA), May 7–10, 2007, Covington, Kentucky, USA.

Sushil, S., Batra, V.S., 2006. Analysis of fly ash heavy metal content and disposal in three thermal power plants in India. Fuel 85, 2676–2679.

Swaine, D. Trace Elements in Coal. Butterworths, London, 1990, 292 pp.

Swaine, D.J., 2000. Why trace elements are important. Fuel Processing Technology 65–66, 21–33.

Taylor, J.C., 1991. Computer programs for standardless quantitative analysis of minerals using the full powder diffraction profile. Powder Diffraction 6, 2–9.

Valentim, B., Lemos de Sousa, M.J., Abelha, P., Boavida, D., Gulyurtlu, I., 2006. The identification of unusual microscopic features in coal and their derived chars: Influence on coal fluidized bed combustion. International Journal of Coal Geology 67, 202–211.

Valentim, B., Hower, J.C., Flores, D., Guedes, A., 2009. Laminar calcite aggregates formation in the fly ash light fraction. World of Coal Ash (WOCA). Lexington, Kentucky, USA. International Ash Utilization Symposia and the World of Coal Ash conference, http://whocares.caer.uky.edu/wasp/AshSymposium/AshLibraryAuthors.asp#V, accessed 6 October 2009.

Valkovic, V., 1983. Trace elements in coal. CRC Press., Inc., Boca Raton, Florida, Vol. II, 281 pp.

Vassilev, S.V., Vassileva, C.G., 1995. Methods for Characterization of Composition of Fly Ashes from Coal-Fired Power Stations: A Critical Overview. Energy & Fuels 19, 1084–1098.

Vassilev, S.V., Vassileva, C.G., 1996a. Mineralogy of combustion wastes from coal-fired power stations. Fuel Processing Technology 47, 261–280.

Vassilev, S.V., Vassileva, C.G., 1996b. Occurrence, abundance and origin of minerals in coals and coal ashes. Fuel Processing Technology 48, 85–106.

Vassilev, S.V., Vassileva, C.G., 2005. Methods for Characterization of Composition of Fly Ashes from Coal-Fired Power Stations: A Critical Overview. Energy & Fuels 19, 1084–1098.

Vassilev, S., Vassileva, C., 2007. A new approach for the classification of coal fly ashes based on their origin, composition, properties, and behavior. Fuel 86, 1490–1512.

Ward, C.R., 2002. Analysis and significance of mineral matter in coal seams. International Journal of Coal Geology 50, 135–168.

Ward, C.R., French, D., 2006. Determination of glass content and estimation of glass composition in fly ash using quantitative X-ray diffractometry. Fuel 85, 2268–2277.

Yan, R., Gauthier, D., Flamant, G., 2001. Partitioning of Trace Elements in the Flue Gas from Coal Combustion. Combustion and Flame 125, 942–954.

Yudovich, Y., Ketris, M., Mertz, A., 1985. Trace Elements in Coal. Nauka, Leningrad, 239 pp. (in Russian).